Drift-Alfvén wave mediated particle transport in an elongated density depression

Stephen Vincena[a] and Walter Gekelman
Department of Physics and Astronomy, University of California at Los Angeles, Los Angeles, California 90095

(Received 14 November 2005; accepted 17 May 2006; published online 14 June 2006)

Cross-field particle transport due to drift-Alfvén waves is measured in an elongated density depression within an otherwise uniform, magnetized helium plasma column. The depression is formed by drawing an electron current to a biased copper plate with cross-field dimensions of 28 $\times 0.24$ ion sound-gyroradii $\rho_s = c_s/\omega_{ci}$. The process of density depletion and replenishment via particle flux repeats in a quasiperiodic fashion for the duration of the current collection. The mode structure of the wave density fluctuations in the plane perpendicular to the background magnetic field is revealed using a two-probe correlation technique. The particle flux as a function of frequency is measured using a linear array of Langmuir probes and the only significant transport occurs for waves with frequencies between 15%–25% of the ion cyclotron frequency (measured in the laboratory frame) and with perpendicular wavelengths $k_\perp \rho_s \sim 0.7$. The frequency-integrated particle flux is in rough agreement with observed increases in density in the center of the depletion as a function of time. The experiments are carried out in the Large Plasma Device (LAPD) [Gekelman *et al.*, Rev. Sci. Instrum. **62**, 2875 (1991)] at the Basic Plasma Science Facility located at the University of California, Los Angeles. © *2006 American Institute of Physics*.
[DOI: 10.1063/1.2211087]

In magnetized plasmas, gradients in the equilibrium density or pressure lead universally to the generation of drift waves.[1] These low-frequency waves convect heat and particles across magnetic field lines and are therefore paramount to understanding containment of magnetized plasmas, especially in devices aimed at the eventual production of a fusion reactor. This importance has spawned a long history of experiments in Q-machines,[2] arc jets,[3] torroidal devices,[4,5] and helicon plasmas.[6] Besides global gradients which affect confinement, it is increasingly observed that narrow pressure structures exist within what would otherwise be characterized as a uniform background magnetized plasma. By narrow, it is meant that the structures have cross-field size on the order of the largest of the physical scaling lengths: the ion cyclotron radius $\rho_i = v_{Ti}/\omega_{ci}$, the electron inertial length $\delta = c/\omega_{pe}$, or the ion sound-gyroradius $\rho_s = c_s/\omega_{ci}$. Here v_{Ti} is the ion thermal velocity, ω_{ci} is the ion-cyclotron frequency, c is the speed of light, ω_{pe} is the electron plasma frequency, and c_s is the ion sound speed. Along the magnetic field, these structures may extend hundreds or thousands of these lengths. Such structures are common in the Earth's auroral ionosphere.[7,8]

In laboratory experiments, tube-like density depressions have been passively created[9] using a solid copper disk placed in front of the cathode in a cathode-anode discharge. This disk blocked primary electrons and inhibited plasma production along field lines intersecting the disk. The authors documented the spontaneous growth of drift-Alfvén waves within these striations, but did not observe a significant particle transport due to the waves. In this study, an elongated density trough is created in the main body of a cathode-anode discharge using the technique of current collection to deplete the pre-existing plasma. This active technique forms deep density depressions which allow the study of cross-field particle transport due to the drift-Alfvén waves. In addition, such elongated density cavities in the presence of electron currents may better model those observed in the ionosphere and the low-frequency waves within them.[10]

The experiment is performed in the upgraded Large Plasma Device (LAPD) (Ref. 11) at the University of California, Los Angeles. The device [shown schematically in Fig. 1(a)] is a stainless steel cylindrical vacuum chamber (length=20.8 m, main diameter=1 m). There is a solenoidal, dc magnetic field $\mathbf{B}_0 = B_0\hat{z}$, here 750 Gauss. The device is backfilled with helium at pressures of approximately 1×10^{-4} Torr. The plasma source is an 11 ms discharge between a hot, oxide-coated nickel cathode and a molybdenum mesh anode, and is repeated once per second. The cathode-anode separation is 52 cm, leaving the remainder of the device with zero net current. The plasma diameter is 40 cm (full width at half maximum) and its peak density is $(2.5 \pm 0.3) \times 10^{12}$ cm^{-3}, measured using a density profile from a swept Langmuir probe together with a 56 GHz microwave interferometer. The electron temperature T_e from the swept probe is (5.5 ± 0.5) eV. Although not measured during this experiment, the ion temperature T_i is estimated from previous experiments under similar conditions to be (1.0 ± 0.5) eV. This estimate is made using both Fabry-Perot interferometry and measurements of the shear Alfvén wave phase velocity near the ion cyclotron frequency.[12] In the background plasma, the physical scale lengths are $\rho_i = 0.27$ cm, $\delta = 0.34$ cm, and $\rho_s = 0.64$ cm.

[a]Electronic mail: vincena@physics.ucla.edu

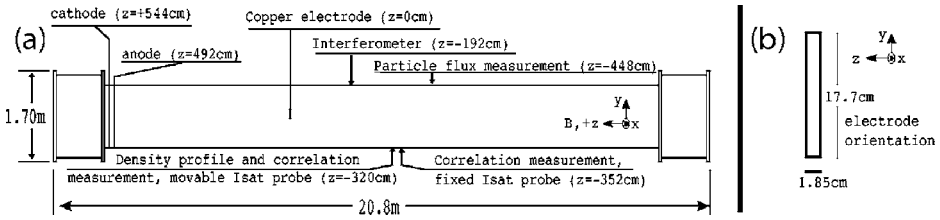

FIG. 1. (a) Schematic of the device and axial locations of the various measurements. (b) Orientation and dimensions of the plate electrode; its thickness is 0.15 cm in the x direction. The origin of the experimental coordinate system is the center of mass of the plate.

There are three main diagnostics for this experiment. The first is a double-sided, planar Langmuir probe with size approximately equal to ρ_i. The normal of one probe face is directed parallel to the background magnetic field, and the other antiparallel. Both faces are biased (with respect to the chamber wall) to collect ion saturation current. The signals from both faces are digitized, averaged, and calibrated using the microwave interferometer to yield the local background density and its fluctuations; this assumes that the variation is due to n rather than T_e.

The second diagnostic uses a pair of such planar probes to measure the mode structure of density fluctuations using a cross correlation technique.[13] One probe is fixed in space while the other (displaced in z) moves in the xy plane under computer control. The mode structure in the plane of the moving probe is obtained from $\tilde{n}_m(\omega)/n_0 = n_{m,\mathrm{rms}}(\omega)\cos(\theta_{fm})/n_0$, where $\tilde{n}_m(\omega)$ is the amplitude and phase of the density fluctuation as a function of frequency, n_0 is the background plasma density, $n_{m,\mathrm{rms}}(\omega)$ is the rms value of the density fluctuation at that frequency, and θ_{fm} is the cross phase between the fixed and moving probe signals calculated using fast Fourier transforms. Subscripts f and m label, respectively, the fixed and moving probe. An ensemble of 30 plasma discharges is collected at each spatial location.

A final diagnostic is used to measure the cross-field particle flux Γ due to coherent fluctuations in density $\tilde{n}$ and electric field $\tilde{E}$. This flux can be computed[14] from

$$\Gamma(\omega) = (c/B_0)\tilde{n}_{\mathrm{rms}}(\omega)\tilde{\phi}_{rms}(\omega)|\gamma_{n\phi}(\omega)|k_y(\omega)\sin[\theta_{n\phi}(\omega)], \tag{1}$$

where $\gamma_{n\phi}$ is the complex coherency between $\tilde{n}$ and $\tilde{\phi}$, $\theta_{n\phi}$ is the cross-phase between $\tilde{n}$ and $\tilde{\phi}$, k_y is the perpendicular wave number, and the electrostatic approximation is used: $\tilde{E}_y = -ik_y\tilde{\phi}$. The measurement is made using a "flux probe," which is a linear array of Langmuir probes (see the inset to Fig. 7). The array is aligned along the y axis with a tip separation of $\Delta y = 5.9\times10^{-2}$ cm. The center tip is located at $(x,y)=(1.25,0)$ cm, and is biased to collect ion saturation current while the remaining tips float electrically, and all signals are referenced to the chamber wall. The center tip, along with the microwave interferometer, yields $\tilde{n}_{\mathrm{rms}}$; $\tilde{\phi}_{\mathrm{rms}}$ is the averaged rms value from the two floating tips closest to the center tip; $\gamma_{n\phi}$ and $\theta_{n\phi}$ are calculated from the cross- and autospectra between $\tilde{n}$ and the two nearest $\tilde{\phi}$ signals (which are again averaged to give values at the center tip); finally, the cross-phase between the bottom-most tip and the other five floating tips is plotted as a function of tip separation and the slope of a linear (least-square) fit yields k_y.

To create the density depression, an electron current sheet is produced by inserting a copper plate into the background plasma and applying to it, at $t=0$, a +85 V pulse relative to the vacuum chamber via a transistor-switched capacitor bank until $t=3$ ms. The main plasma breakdown occurs at $t=-7$ ms and steady state background conditions are achieved by $t=-2$ ms. The dimensions of the plate are $l_x=0.15$ cm $\times l_y=17.7$ cm $\times l_z=1.85$ cm. The plate is aligned such that its length l_z extends along the z direction as shown in Fig. 1(b). The center of mass of the plate also defines the zero of the experimental coordinate system. The bias applied to the electrode depletes plasma electrons along the connecting field lines, and the result is a long, field-aligned density "trough" within the background plasma. A profile of the density depression (averaged over 30 plasma discharges) at time $t=32$ μs is shown in Fig. 2. The density depression at this time is roughly 1 cm wide with a depth of 50% of the background density. This average central density represents a balance between the collection of electrons at the electrode and cross-field scattering and replenishment along the length of the device.

The current drawn to the electrode as a function of time for a single plasma discharge is displayed in Fig. 3(a) while Fig. 3(b) shows the time series of the density measured in the gradient region of the density profile $(x,y,z)=(1,0,-352)$ cm for the same discharge. The current appears modulated in a periodic fashion with more current drawn at times

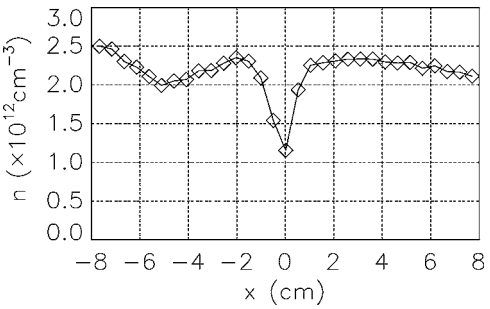

FIG. 2. Profile of the density depression at time $t=32$ μs after the bias pulse is applied to the plate electrode. The profile is obtained from ion saturation current measurements at each location along the line $y=0$, and averaged over 30 plasma discharges. The measurement uncertainty is ±10% and assumes a constant background electron temperature of 5.5 eV. The unbiased electrode produces a much shallower depression (within 10% of the background) at $x=0$.

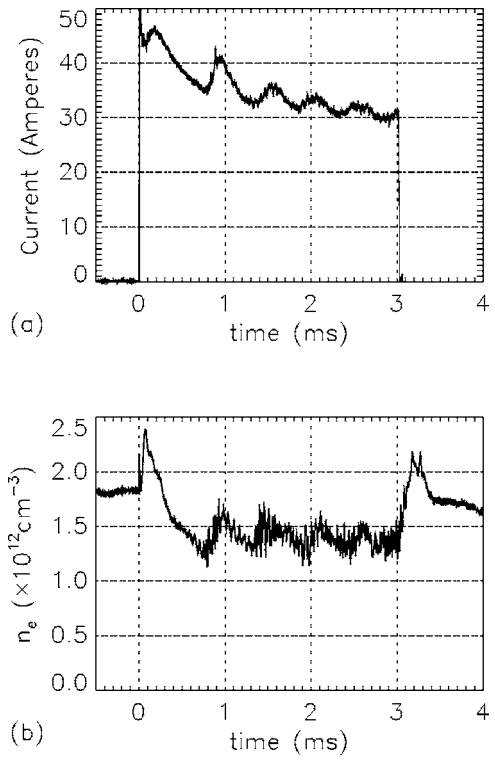

FIG. 3. (a) Time series of the current drawn to the electrode (data from a single plasma shot). (b) Ion saturation current time series for the same shot measured in the density gradient $(x,y,z)=(1.0,-2.0,-352)$ cm. The voltage applied by the pulser circuit is constant in time. The oscillations are produced by the plasma. The transformer used to measure the current has a droop of 4% per millisecond.

correlated with increases in plasma density in the current sheet. Higher frequency density fluctuations are also apparent at times when the net density is increasing at this location. These higher frequency fluctuations are localized within the gradient region of the density profile which suggests they be classified as drift waves; or, more specifically[9] as drift-Alfvén waves since the plasma beta scaled by the ion-to-electron mass ratio is greater than unity. Here, $\beta=(8\pi nT/B_0^2)(m_i/m_e)=7.2$. The spectra of density and floating potential fluctuations are measured in the gradient using the flux probe and are presented in Fig. 4. In the absence of dissipation, the fluctuations should obey a Boltzmann relationship which, in the linear regime, gives $\delta n_e/n_0 \approx e\delta\phi/T_e$. This relationship holds for the data for frequencies roughly above $0.2f_{ci}$. The deviation at lower frequencies indicates the presence of dissipation, hence a destabilization mechanism for the mode growth.[15] The details of the dissipation are not explored here, but parallel resistivity is a likely candidate since the electron-ion Coulomb collision frequency is 3.5 times larger than the angular ion-cyclotron frequency.

The spatial mode structure of the density fluctuations is measured in the xy plane using the cross-correlation technique described earlier. The fixed probe is placed in the density gradient $(x_f,y_f,z_f)=(-0.5,-2.5,-352)$ cm while the moving probe is in the plane $z_m=-320$ cm. The reconstruction is presented in Fig. 5, for a single frequency $f=0.19f_{ci}$ corresponding to the local maximum in the power spectra of Fig. 4. Here, the ion cyclotron frequency $f_{ci}=\omega_{ci}/2\pi$ is

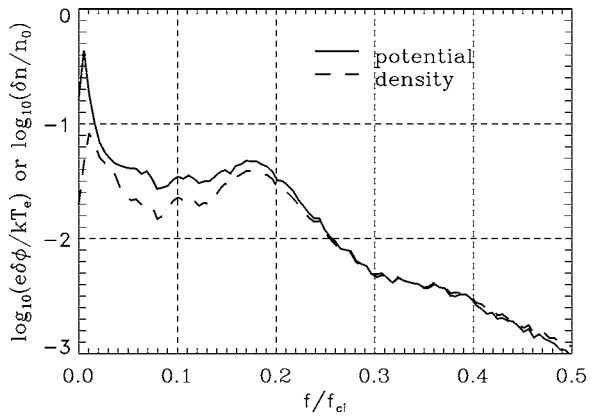

FIG. 4. Spectra of density and floating potential amplitude fluctuations. Density fluctuations are scaled by the background density and the potential fluctuations are scaled by the electron temperature.

288 Hz. The data are color-coded, with red (blue) being a positive (negative) density perturbation, and green is zero. Initial measurements place the parallel wavelength of the fluctuations at 600 cm±400 cm, which is a minimum of six times the axial probe separation. When the phase of the data is evolved as $\cos(\theta_{fm}-\omega t)$, the phase fronts follow the density contours (shown as black lines) in a clockwise sense,

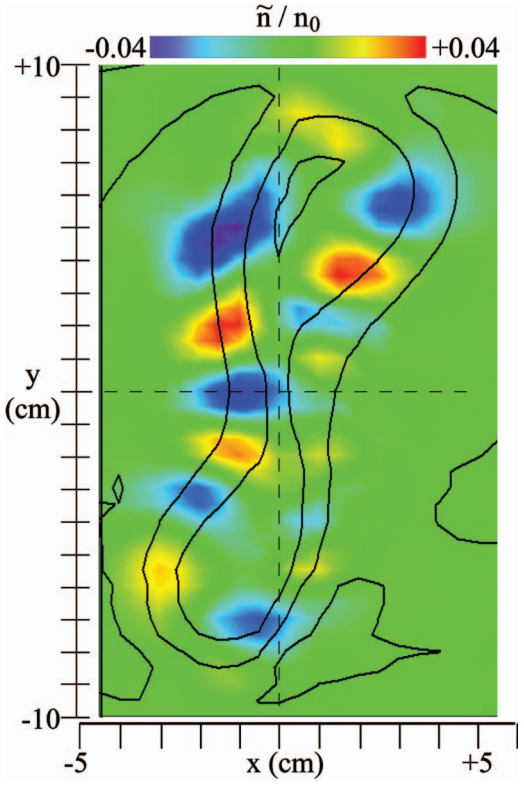

FIG. 5. (Color) Two-dimensional wave mode structure of density fluctuations, notch-filtered at frequency $f=0.19f_{ci}$. This frequency corresponds to the maximum cross-field particle flux. The moving probe samples 21 positions in x and 41 positions in y with equal spacing of 0.5 cm. The black lines are density contours. The magnetic field points out of the page and the propagation direction of the wave is along the density contours in the clockwise (electron diamagnetic drift) direction.

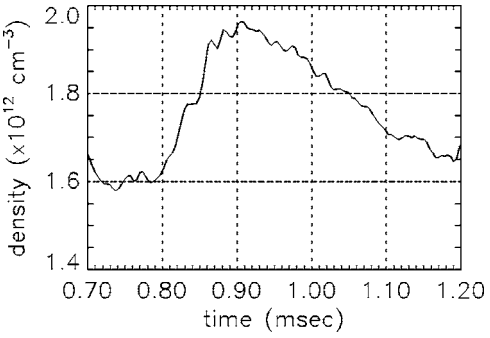

FIG. 6. Density as a function of time measured with a Langmuir probe biased to collect ion-saturation current at $(x,y,z)=(0,0,-448)$ cm. The time series is plotted starting at 0.7 ms after the turn on of bias voltage to the plate located at the origin. The density is averaged over an ensemble of 128 plasma discharges. The measurement assumes a constant electron temperature of 5.5 eV.

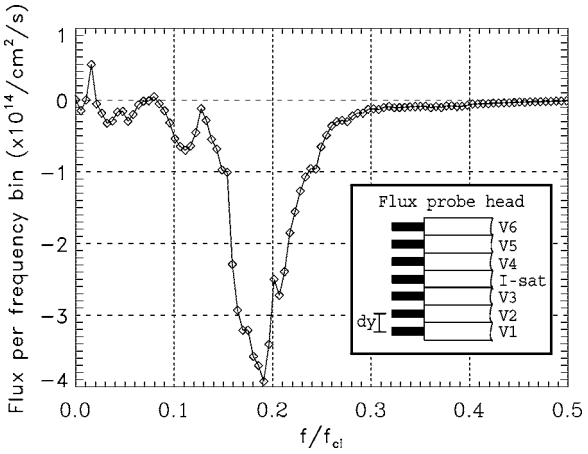

FIG. 7. Frequency spectrum of the particle flux in the laboratory frame, with insert of the flux probe used for the measurement. The frequency integrated particle flux is $\Gamma=-5.5\times10^{15}$ cm^{-2} s^{-1}.

which is the direction of the electron diamagnetic drift, and consistent with the drift wave identification of the mode.

The average density within the depression does not reach a steady state as would be expected from a balance of plasma depletion and diffusion; rather, the density gradient is reduced in bursts which are well correlated with the drift wave fluctuations. Figure 6 shows a section of the time history of the density at $(x,y,z)=(0,0,-448)$ cm starting at time $t=0.7$ ms. Note that at this time, the full width at half depth of the density trough is 2.5 cm (slightly wider than in Fig. 2). The density is averaged over 128 plasma discharges to render the net increase in density apparent rather than the fluctuations. In this averaged sense, the particle flux Γ for $x>0$ necessary to account for the increased density is $\Gamma=-\frac{1}{2}\Delta n\Delta x/\Delta t$. Where the factor of one-half presumes that there is an equal and opposite flux of particles from $x<0$, and the minus sign indicates the flux is in the $-\hat{x}$ direction. For Δx we use 1.25 cm which is the half width of the depression and the location of peak density and floating potential fluctuation amplitudes along the positive x axis. Using $\Delta t=100$ μs, $\Delta n=3.5\times10^{11}$ cm^{-3} gives the average particle flux for $x>0$ of $\Gamma=-2.2\times10^{15}$ cm^{-2} s^{-2}.

To compare, the particle flux due to density and electric field fluctuations is measured using the linear array described earlier and the flux from Eq. (1) calculated using an ensemble average of 128 plasma discharges; the result is plotted in Fig. 7. Since Γ is primarily negative, the flux is directed to fill in the density depression. The maximum inward flux occurs for $f/f_{ci}=0.19$, with a perpendicular wave number of $k_y\rho_s=-0.69$. Overall, the range in significant net particle transport occurs in a narrow frequency band: $0.15<f/f_{ci}<0.25$, corresponding to wave numbers $-0.55\geqslant k_y\rho_s\geqslant-0.81$. The frequency integrated particle flux, found by summing the frequency bins, is -5.5×10^{15} cm^{-2} s^{-1}. This is a factor of 2 larger than the value computed from the time-varying central density, but this flux was measured at a single x location—that of peak fluctuation amplitudes—which makes it an upper bound. A full profile of the flux is needed for a more accurate comparison.

In summary, a biased electrode has been used to create a field-aligned depletion of plasma density which gives rise to drift-Alfvén waves which, in turn, are responsible for cross-field particle transport that relax the gradient. The rate of filling of the central density is consistent with measurements of the $\tilde{E}\times B_0$ particle flux made using a linear probe array. In future publications, we will discuss the physics of the formation of the density cavity including the open question of ion heating, as well as a detailed investigation of the wave dispersion and particle transport.

This work was funded jointly by the DOE and NSF under Grant No. DE-FG02-03R54717, and the work was carried out at the Basic Plasma Science Facility which is funded by a NSF-DOE cooperative agreement, under Grant No. PHY-0075916.

[1] W. Horton, Rev. Mod. Phys. **71**, 735 (1999).
[2] H. W. Hendel, T. K. Chu, and P. A. Politzer, Phys. Fluids **11**, 2426 (1968).
[3] J. T. Tang and N. C. L. Luhmann Jr., Phys. Fluids **19**, 1935 (1976).
[4] E. D. Fredrickson and P. M. Bellan, Phys. Fluids **28**, 1866 (1995).
[5] R. V. Bravenec, K. W. Gentle, B. Richards, D. W. Ross, D. C. Sing, A. J. Wooton, D. L. Brower, N. C. L. Luhmann Jr., W. A. Peebles, C. X. Yu *et al.*, Phys. Fluids A **4**, 2127 (1992).
[6] C. Schröder, O. Grulke, T. Klinger, and V. Naulin, Phys. Plasmas **11**, 4249 (2004).
[7] P. M. Kintner, J. Vago, S. Chesney, R. L. Arnoldy, K. A. Lynch, and C. J. P. T. E. Moore, Phys. Rev. Lett. **68**, 2448 (1992).
[8] A. I. Eriksson, B. Holback, P. O. Dovner, R. Bostrom, G. Holmgren, M. Andre, L. Eliasson, and P. M. Kintner, Geophys. Res. Lett. **21**, 1843 (1994).
[9] J. E. Maggs and G. J. Morales, Phys. Plasmas **4**, 290 (1997).
[10] C. C. Chaston, V. Genot, J. W. Bonnell, C. W. Carlson, J. P. McFadden, R. E. Ergun, R. J. Strangeway, E. J. Lund, and K. J. Hwang, J. Geophys. Res. **111**, A03206 (2006).
[11] W. Gekelman, H. Pfister, Z. Lucky, J. Bamber, D. Leneman, and J. Maggs, Rev. Sci. Instrum. **62**, 2875 (1991).
[12] S. Vincena, W. Gekelman, and J. Maggs, Phys. Plasmas **8**, 3884 (2001).
[13] J. S. Bendat and A. G. Piersol, *Random Data: Analysis and Measurement Procedures*, 3rd ed. (Wiley, New York, 2000).
[14] A. J. Wootton, B. A. Carreras, H. Matsumoto, K. McGuire, W. A. Peebles, C. P. Ritz, P. W. Terry, and S. J. Zweben, Phys. Fluids B **2**, 2879 (1990).
[15] J. C. Perez, W. Horton, K. Gentle, W. L. Rowan, K. Lee, and R. B. Dahlburg, Phys. Plasmas **13**, 032101 (2006).